

# REPORT DOCUMENTATION PAGE

Form Approved  
GSA No. 0704-0188

(2)

Public reporting burden for this edition of information is estimated to average 1 hour per response, including the time for reviewing instructions, searching existing data sources, gathering and maintaining the data needed, and completing and reviewing the collection of information. Send comments regarding this burden estimate or any other aspect of this collection of information, including suggestions for reducing this burden, to Washington Headquarters Service, Directorate for Information Operations and Reports, 1215 Jefferson Davis Highway, Suite 1204, Arlington, VA 22202-4302, and to the Office of Management and Budget, Paperwork Reduction Project (0704-0188), Washington, DC 20503.

1. AGENCY USE ONLY (Leave blank)		2. REPORT DATE 11/30/93		3. REPORT TYPE AND DATES COVERED Ann. Tech. 12/1/92-11/30/93	
4. TITLE AND SUBTITLE (U) Computer Simulation of Molecular Interactions in Supercritical Solvents				5. FUNDING NUMBERS PE - 61102F PR - 2308 SA - BS G - F49620-93-I-0040	
6. AUTHOR(S)  P.G. Debenedetti				7. PERFORMING ORGANIZATION REPORT NUMBER AFOSR-TR 94 0033	
7. PERFORMING ORGANIZATION NAME(S) AND ADDRESS(ES) Princeton University Department of Chemical Engineering Princeton, NJ 08544-5263				8. PERFORMING ORGANIZATION REPORT NUMBER	
9. SPONSORING/MONITORING AGENCY NAME(S) AND ADDRESS(ES) AFOSR/NA 110 Duncan Avenue, Suite B115 Bolling AFB DC 20332-0001				10. SPONSORING/MONITORING AGENCY REPORT NUMBER	
11. SUPPLEMENTARY NOTES					
12a. DISTRIBUTION/AVAILABILITY STATEMENT  Approved for public release; distribution is unlimited				12b. DISTRIBUTION CODE	
13. ABSTRACT (Maximum 200 words)  Integral equation calculations were performed on two model supercritical mixtures: naphthalene in carbon dioxide (non-volatile solute; attractive mixture) and neon in xenon (volatile solute; repulsive mixture). Both systems were studied at high dilution, at supercritical temperature, and over a broad range of densities. The attractive system exhibited significant short-ranged solvent enrichment around the solute. The difference between the solvent density averaged over three solvation shells, and the bulk solvent density was found to be more pronounced between 50 and 80% of the solvent's critical density. In contrast, the repulsive system exhibited local solvent depletion near the solvent's critical point. The extent of the solvation region responsible for determining the solute's chemical potential varies between three and five solvent diameters for the attractive mixture, with the maximum occurring near the solvent's critical density. At 60% of the solvent's critical density, the local concentration of naphthalene molecules around each other is almost ten times higher than in the bulk. Dynamic simulations of pyrene in carbon dioxide revealed insignificant solute-solute aggregation. The mean lifetime of transient solute dimers, roughly 0.8 picoseconds, was found not to change even when the bulk density was varied by a factor of four.					
14. SUBJECT TERMS Molecular dynamics simulation; integral equation calculations; molecular interactions in supercritical solvents.				15. NUMBER OF PAGES 27	
16. PRICE CODE				17. SECURITY CLASSIFICATION OF ABSTRACT	
17. SECURITY CLASSIFICATION OF REPORT Unclassified		18. SECURITY CLASSIFICATION OF THIS PAGE Unclassified		19. SECURITY CLASSIFICATION OF ABSTRACT Unclassified	
20. LIMITATION OF ABSTRACT UL					

NSN 7540-01-280-5500

Standard Form 298 (890'04 Draft)  
Prescribed by ANSI Std. Z39-18  
298-01

AD-A274 977



94-02660

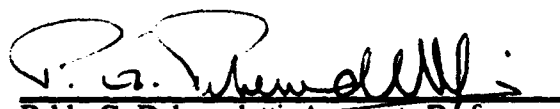
**Best  
Available  
Copy**

**Annual Technical Report Under  
AFOSR Grant No. F49620-93-1-0040**

**Air Force Office of Scientific Research**

**for the Period December 1, 1992 - November 30, 1993**

**COMPUTER SIMULATION OF MOLECULAR INTERACTIONS IN  
SUPERCRITICAL SOLVENTS**

  
Pablo G. Debenedetti, Associate Professor  
Principal Investigator

Department of Chemical Engineering  
Princeton University  
Princeton, NJ 08544-5263

**94 1 26 105**

## 1. Introduction

A fluid is said to be supercritical when its temperature and pressure are simultaneously higher than their critical point values (McHugh and Krukonis, 1986). In practice, though, the term supercritical is used to describe fluids within the relatively narrow range of temperatures and pressures ( $1 < T/T_c < 1.1$ ;  $1 < P/P_c < 2$ ), where subscript c denotes critical point values (Brennecke and Eckert, 1989). It is within this region that most property changes involved in the transition from a dilute gas to a dense fluid occur. Consequently, the thermophysical properties of supercritical fluids exhibit high rates of change with respect to temperature and pressure. Not all properties change at the same rate; hence the combination of thermophysical properties of supercritical fluids is quite unique. For example, supercritical fluids have liquid-like densities, kinematic viscosities that are lower than those of liquid metals, compressibilities that can be arbitrarily higher than for an ideal gas, and viscosities that are intermediate between gas- and liquid-like (Debenedetti and Reid, 1986).

Dilute mixtures in which the solvent is supercritical can be classified into three categories: attractive, weakly attractive, and repulsive (Petsche and Debenedetti, 1991). The first are of technological interest, as nearly all applications of supercritical fluids involve attractive solutions. In such a class of binary mixture, there is long-ranged solvent enrichment around the solute molecules in the vicinity of the solvent's critical point, solubility enhancement, and the solute's partial molar volume and enthalpy are large and negative, diverging to  $-\infty$  at the solvent's critical point in the limit of infinite dilution. Attractive behavior occurs generally when the solute is larger than the solvent and has a correspondingly larger characteristic interaction energy. In practical terms, this generally means a low-volatility solute dissolved in a supercritical solvent. Repulsive solutions are mainly of theoretical interest, although experiments with repulsive supercritical solutions have been reported (Biggerstaff and Wood, 1988 a,b). In a repulsive mixture, there is long-ranged solvent depletion around the solute molecules in the neighborhood of the solvent's critical point, and the solute's partial molar volume and enthalpy are large and positive, diverging to  $+\infty$  at the solvent's critical point in the limit of infinite dilution. Repulsive behavior occurs when the solvent is larger than the solute and has a correspondingly larger characteristic interaction energy. The microstructure around solute molecules tends to be solvent-rich in the attractive case, and solvent-lean for repulsive binaries.

DTIC QUALITY INSPECTED 8

For	
I	<input checked="" type="checkbox"/>
d	<input type="checkbox"/>
len	<input type="checkbox"/>
Distribution/	
Availability Codes	
Dist	Avail and/or Special
A-1	

A large body of experimental (Kim and Johnston, 1987a,b; Johnston et al., 1989; Brennecke and Eckert, 1989; Brennecke et al., 1990 a,b; Betts et al., 1992 a,b; Sun et al., 1992), theoretical (Wu et al., 1990; Munoz and Chimowitz, 1992; Tom and Debenedetti, 1993), and computational (Petsche and Debenedetti, 1989; Knutson et al., 1992; O'Brien et al., 1993) evidence suggests that in dilute supercritical mixtures of practical interest the local environment surrounding solute molecules (microstructure) differs appreciably from the bulk. Thus, an improved understanding of the structure and dynamics of the local environment around solute species could well lead to the tailoring of specific solvent environments for targeted separations or reactions.

## **2. Objective**

Potential applications of supercritical fluids range from their use as highly selective solvents for difficult separations (Brennecke and Eckert, 1989), to materials processing and particle formation (Tom and Debenedetti, 1991). The actual implementation of some of these promising technologies has been hampered by a lack of understanding of key aspects of the behavior of fluids and their mixtures at supercritical conditions, such as molecular interactions and solvation mechanisms, transport properties and reaction kinetics, and mechanisms of nucleation and growth leading to particle formation. The objective of this research is to gain an understanding of the microscopic structure and dynamical behavior of supercritical mixtures, using integral equation calculations and molecular dynamics computer simulations. The quantities of interest include molecular distribution functions, local density augmentation and depletions, solute rotational dynamics, solvation mechanisms and dynamics, dynamics of solute-solute collisions, solute translational diffusion. In this report, we describe integral equation calculations and molecular dynamics simulations of model attractive and repulsive supercritical Lennard-Jones mixtures.

## **3. Status of the Research Effort**

### Integral Equation Calculations

Integral equations are useful for studying dilute supercritical mixtures because arbitrarily low solute mole fractions can be studied at no additional computational cost. The technique only yields structural, thermodynamic information. Two highly dilute binary

supercritical systems were studied: one is attractive and one repulsive. The spherically symmetric Lennard-Jones potential was used in both cases. Potential parameters are listed in Tables I and II. These mixtures have been called naphthalene in carbon dioxide [attractive case; see Cochran and Lee (1989)] and neon in xenon [repulsive case; see Petsche and Debenedetti (1989)]. We use this terminology, although it should be understood that except for yielding reasonable estimates for the pure-component critical temperatures and densities with the parameters listed in Tables I and II, the Lennard-Jones potential is a rudimentary representation of the actual interaction potentials, especially in the attractive case. The basic features of the attractive and repulsive behavior to be discussed below, however, are quite general, and hence independent of the details of the intermolecular potentials.

**Table I. Lennard-Jones Parameters for Naphthalene in CO<sub>2</sub>**

Naphthalene in CO <sub>2</sub>	ij	$\sigma_{ij}$ (Å)	$\sigma_{ij}/\sigma_{22}$	$\epsilon_{ij}/k$ (K)	$\epsilon_{ij}/\epsilon_{22}$
solute-solute	11	6.199	1.634	554.4	2.458
solvent-solvent	22	3.794	1.000	225.5	1.000
solute-solvent	12	4.996	1.317	353.4	1.567

**Table II. Lennard-Jones Parameters for Neon in Xenon**

Neon in Xenon	ij	$\sigma_{ij}$ (Å)	$\sigma_{ij}/\sigma_{22}$	$\epsilon_{ij}/k$ (K)	$\epsilon_{ij}/\epsilon_{22}$
solute-solute	11	2.82	0.697	32.8	0.142
solvent-solvent	22	4.047	1.000	231.0	1.000
solute-solvent	12	3.433	0.848	87.0	0.377

Dimensionless temperatures, densities, and distances are denoted by a superscript \*, and are given by  $T^* = kT/\epsilon_2$ ,  $\rho^* = \rho \sigma_2^3$ , and  $r^* = r/\sigma_2$ , respectively (1 = solute; 2 = solvent). A solute mole fraction of  $10^{-9}$  was used in all the calculations to approximate infinitely dilute conditions. Attractive mixture calculations were done at  $T^* = 1.4$ , and  $0.1 < \rho^* < 0.5$ . Repulsive mixture calculations were done at  $T^* = 1.4$  and  $0.1 < \rho^* < 0.7$ . Using the best estimate of the critical point for a Lennard-Jones fluid ( $\rho_c^* = 0.31$ ;  $T_c^* = 1.31$ ; Smit et al., 1989) this corresponds to a reduced temperature,  $T/T_c = 1.07$  (attractive and repulsive cases), and reduced density ranges ( $\rho/\rho_c$ ) of 0.32 to 1.61 (attractive case) and 0.32 to 2.26 (repulsive case).

Figures 1 and 2 show the solute-solute (11) and solute-solvent (12) pair correlation functions for the attractive mixture. The first peak of the 11 correlation occurs at  $r^* = 1.8$ , and represents the direct contact between naphthalene molecules. This distance corresponds to the well of the 11 potential, which occurs at a separation of 1.83. The maximum peak occurs at a reduced density ( $\rho/\rho_c$ ) of 0.58. A second feature of the solute-solute correlation function is a broad shoulder occurring approximately between  $r^* = 2.3$  and 3 at sub-critical densities. For densities above  $\rho^* = 0.25$ , the shoulder becomes a second peak, whose location ( $r^* = 2.76$ ) suggests a contribution from naphthalene-CO<sub>2</sub>-naphthalene triplets. The minimum between the first two peaks decreases with density: it falls below unity at  $\rho^* = 0.4$ . These calculations provide further evidence of high solute-solute peaks in attractive mixtures (Chialvo and Debenedetti, 1992), especially at sub-critical densities. The solute-solvent (12) correlation (Figure 2) shows a first peak at  $r^* = 1.44$ , representing the direct contact between naphthalene and CO<sub>2</sub> molecules. Note that, contrary to the 11 function, the first peak attains its highest value ( $g_{12} = 3.07$ ) at the lowest density studied here ( $\rho^* = 0.1$ , vs.  $\rho^* = 0.18$  for the  $g_{11}$  maximum peak).

A convenient way of quantifying the local-bulk asymmetry of the distribution of solvent molecules is by integrating the solute-solvent pair correlation function and defining a radially-dependent local density within a sphere of radius  $r$  around a central solute molecule,

$$\langle N_{21}(r) \rangle = \rho_2 \int_0^r 4\pi r'^2 g_{12}(r') dr' \quad (1)$$

$$\rho_{local}(r) = \frac{\langle N_{12}(r) \rangle}{\frac{4\pi}{3} \left[ r^3 - \left( \frac{\sigma_1}{2} \right)^3 \right]} \quad (2)$$

where  $\langle N_{12}(r) \rangle$  is the average number of solvent molecules within a sphere of radius  $r$  centered around a solute molecule, and  $\rho_{local}$  is the average solvent density within the same sphere, but excluding the solute's effective volume. Figure 3 shows the radial and density dependence of  $\rho_{local}$  for the attractive mixture, normalized by the bulk density (so that all curves decay to unity at sufficiently large distances). The radius of the partially hollow sphere within which density augmentation is largest decreases monotonically with density, from  $r^* = 1.84$  at  $\rho^* = 0.1$  to  $r^* = 1.72$  at  $\rho^* = 0.5$ . The maximum density enhancement always occurs within the first solvation shell. However, significant density augmentation persists even up to three solvation shells. At low and near-critical densities, the enhancement persists over large distances away from the solute molecule (for example, at  $\rho^* = 0.2$ ,  $\rho_{local}/\rho_{bulk} = 1.045$  at  $r^* = 8$ ). However, at higher densities, the enhancement decays much more rapidly (e.g., at  $\rho^* = 0.5$ ,  $\rho_{local}/\rho_{bulk} = 1.01$  at  $r^* = 5$ ). This is due to a cancellation between peaks and valleys in the correlation function as liquid-like densities are approached. Thus, we see an augmentation in the solvent's local density that is particularly pronounced at subcritical densities and decreases rapidly at liquid-like densities.

Corresponding calculations are shown in Figures 4, 5 for the repulsive mixture. The solute-solvent pair correlation function shows a marked difference with respect to the corresponding attractive quantity (Figure 2). In the attractive case we see a pronounced first peak that decreases with density, and a shallow first valley. In the repulsive case, we see a mild first peak which increases with density, and a deep first valley. The density and radial dependence of the local density [as defined in (2)] is shown in Figure 5. Note that at  $\rho^* = 0.1$ ,  $\rho_{local}/\rho_{bulk}$  approaches 1.0 monotonically from below. Above this density, the monotonic rise evolves gradually, first into a curve with an inflection point at  $r^* = 1.75$ , and then into a curve with maxima and minima. Minima and inflection points occur between  $r^* = 1.6$  and 1.8 (within the second solvation shell), with the deepest minimum occurring at a density  $\rho^* = 0.3$ . Thus, unlike the case of the attractive mixtures (where the most pronounced local density enhancements are found at substantially subcritical densities), repulsive mixtures show the greatest density depletion close to the critical density. Correlation holes such as the one shown in Figure 5 are unusual. They occur here



not because of packing constraints (the usual cause of correlation holes in branched and chain molecules), but because of competitive attractions ( $\epsilon_{22} \gg \epsilon_{12}$ ) at moderate density. Note the rapid disappearance of repulsive behavior at high density.

Integral equations provide a link between microstructure and thermodynamics because they allow the calculation of chemical potentials. Specifically, we are interested in the solute's fugacity coefficient,  $\phi_1$ , defined by

$$\mu_1 = kT \ln \left[ \frac{y_1 \phi_1 P \Lambda_1^3}{kT} \right] \quad (3)$$

where  $\mu_1$  is the solute's chemical potential,  $y_1$ , its mole fraction in the fluid phase,  $P$  is the pressure,  $\Lambda_1$  is the solute's deBroglie wavelength, and  $k$  is Boltzmann's constant. The fugacity coefficient, in other words, is the proportionality constant between partial pressure and fugacity

$$f_1 = y_1 P \phi_1 \quad (4)$$

This quantity is of fundamental importance for solubility calculations. In particular, it is related to  $y_1$ , the equilibrium mole fraction of a pure, incompressible, non-volatile solute in a fluid phase by

$$\phi_1^{-1} = \frac{y_1 (P / P_{vap})}{\exp[P v_{solid} / kT]} \quad (5)$$

where  $P_{vap}$  is the solute's vapor pressure at the given temperature, and  $v_{solid}$ , its molecular volume in the condensed (solid) phase. The numerator in (5) is the ratio of actual to ideal-gas-predicted solubility (enhancement factor). The denominator is called the Poynting correction factor. The enhancement factor changes by several orders of magnitude as the

fluid is compressed isothermally from a low-density gas to supercritical densities. In contrast, the Poynting correction is quite insensitive to pressure (e.g., at 300K, and for a typical  $v_{\text{solid}} = 1.66 \times 10^{-28} \text{ m}^3$ , the Poynting factor changes from 1 to 1.49 in going from 1 to 100 bar). Thus, the reciprocal of the solute's fugacity coefficient is directly proportional to the enhancement in solubility with respect to ideal gas conditions at the given temperature and pressure. The solute's fugacity coefficient and its reciprocal are both plotted versus bulk density for the attractive mixture in Figure 6. The extreme sensitivity to changes in density is obvious.

To examine the relationship between solubility enhancement and microstructure, we use a variable radial cutoff,  $R$ , in the calculation of the integrals that lead to the solute's chemical potential (or, equivalently, to its fugacity). Beyond  $R$ , the mixture is assumed to be uniform ( $g_{ij} = 1$ ). Within  $R$ , pair correlation functions from integral equation calculations were used. This calculation provides a direct measure of the extent of the region surrounding the solute molecules that contributes to that species' fugacity coefficient, and hence to its solubility. The radial cutoff required in the evaluation of the integrals in order to obtain a quantity equal to 99.5, 99, and 98% of the true (bulk) fugacity coefficient is plotted in Figure 7. There is a noticeable dependence of the cutoff upon bulk density. As the critical density is approached, larger cutoffs are required. It is obviously the microstructure ( $3 < R^* < 5.5$ , or  $11 \text{ \AA} < R < 20 \text{ \AA}$ ) that determines the solute's fugacity coefficient. While other thermodynamic quantities in dilute supercritical solutions (such as the solute's partial molar properties) are determined by long-ranged correlations in the compressible near-critical region, we find that it is only the microstructure around the solute (10-20  $\text{\AA}$ ) that affects solvation, and hence solubility.

The above-described integral equation calculations have allowed the investigation of the spatial distribution of solvent and solute molecules in two binary Lennard-Jones mixtures: one, attractive, with potential parameters chosen to represent naphthalene in carbon dioxide; the other, repulsive, with potential parameters chosen to represent neon in xenon. In particular, integral equations provide a direct link between microstructure (radial distribution functions) and thermodynamics (chemical potentials and solubility). Accordingly, we have placed emphasis in understanding how differences between local and bulk conditions around solute molecules influence bulk thermodynamic behavior. As with other types of mixtures, the microstructure is important in determining the solute's solubility in a given solvent, and hence we also investigated its relationship to fugacity coefficients. What is unique to supercritical mixtures is the coexistence of widely different

relevant length scales, with microstructure controlling solubility, and long-ranged, critically-driven fluctuations controlling the temperature and pressure derivatives of solubility. In the attractive mixture, the microstructure is found to be solvent-rich with respect to the bulk. This enrichment persists even when the solvent density is averaged over three solvation shells, and is particularly pronounced in the density range  $0.5 < \rho/\rho_c < 0.8$ . At higher densities, packing constraints become progressively important, the pair correlation function gradually acquires liquid-like oscillatory character, and density enhancement in one solvation shell (peaks) are canceled by depletions in the successive one (valleys). While the magnitude of the enhancement in the first solvation shell is unrelated to proximity to criticality, the persistence length of this density perturbation is directly affected by the growth of the correlation length. Thus, the local density, when averaged over two or three solvation shells, is the result of the subtle interplay between specific (short-range) and universal (long-ranged) effects. The solvation region around the attractive solute was found to be a sensitive function of bulk density, and varied between 11 and 20 Å (3 and 5.5 solvent diameters), with the maximum occurring near the solvent's critical density. The repulsive microstructure was found to be solvent-lean. Correlation holes appear as a result of competitive attractions. Deviations between local solvent density (averaged over two solvation shells) and bulk conditions are particularly pronounced near the solvent's critical density.

### Molecular Dynamics Simulations

In order to investigate the dynamic, time-dependent behavior that corresponds to the above-discussed microstructural features, we conducted a series of molecular dynamics simulations on a model attractive Lennard-Jones mixture. Potential parameters are listed in Table III.

**Table III. Lennard-Jones Parameters for Pyrene in CO<sub>2</sub>**

Pyrene in CO <sub>2</sub>	ij	$\sigma_{ij}$ (Å)	$\sigma_{ij}/\sigma_{22}$	$\epsilon_{ij}/k$ (K)	$\epsilon_{ij}/\epsilon_{22}$
solute-solute	11	7.140	1.882	662.8	2.942
solvent-solvent	22	3.794	1.000	225.3	1.000
solute-solvent	12	5.467	1.440	386.4	1.715

A mass ratio of  $m_1/m_2 = 4.597$  was used to simulate the pyrene-carbon dioxide system. The simulations were carried out in the canonical ensemble (constant volume,  $V$ ; number of molecules,  $N$ ; and temperature,  $T$ ). A time-step of  $0.004 \sigma_2 \sqrt{m_2 / \epsilon_2}$ , which is equivalent to  $7.355 \times 10^{-15}$  sec., and a 5th-order predictor-corrector scheme with an automated Verlet neighbor list (Chialvo and Debenedetti, 1991) were used to integrate the equations of motion. A sample size and solute mole fraction of 4000 and 0.0025, respectively, were used throughout the study (10 solute, 3990 solvent molecules). The simulation length at the three state points studied so far was 200,000 steps (1471 picoseconds). These are exceptionally long simulations, a requirement imposed by the need to gather good solute-solute statistics in a dilute mixture. Three simulations have been carried out so far, at densities ( $\rho^* = \rho \sigma_2^3$ ) 0.15, 0.31, and 0.6, and at a temperature ( $T^* = kT/\epsilon_2$ ) 1.4. This corresponds to a solvent reduced density range of 0.48 to 1.93, and a solvent reduced temperature of 1.07.

In the course of each simulation we studied solute-solute aggregation statistics. To this end, two solute molecules were considered "bound" at any instant if their centers were within a distance not exceeding  $1.122 \sigma_1$  (location of the solute-solute potential well). The algorithm of Sevvick et al. (1988) was used to determine connectivities, and hence the instantaneous distribution of solute-solute aggregates. Results from these calculations are summarized in Table IV.

**Table IV. Aggregate Statistics and Collision Dynamics for Pyrene-CO<sub>2</sub>**

Observable	$\rho^* = 0.15$	$\rho^* = 0.31$	$\rho^* = 0.60$
$10^{-32}$ coll. rate ( $l^{-1} s^{-1}$ )(a)	$1.16 \pm 0.27$	$1.81 \pm 0.45$	$3.03 \pm 1.24$
$10^{-11}$ k ( $l s^{-1} mol^{-1}$ )(b)	$14.8 \pm 3.5$	$5.41 \pm 1.37$	$2.42 \pm 0.99$
% monomers	$97.27 \pm 0.36$	$98.19 \pm 0.04$	$98.08 \pm 0.48$
% dimers	$2.77 \pm 0.59$	$2.10 \pm 0.28$	$1.79 \pm 0.46$
% trimers	$0.16 \pm 0.10$	-	$0.177 \pm 0.158$
dimer lifetime (ps)	$0.758 \pm 0.045$	$0.781 \pm 0.052$	$0.799 \pm 0.076$
trimer lifetime (ps)	$0.494 \pm 0.292$	-	$0.420 \pm 0.103$

(a) Solute-solute collision rate,  $r$ .

(b) Rate constant for solute-solute collisions,  $k = r/\rho_l^2$

It can be seen that the solute is present overwhelmingly in unassociated form, and that this behavior is unaffected by density. Likewise, the average lifetime of a dimer is quite insensitive to density variations. Figure 8 shows the distribution of dimer lifetimes for the three densities investigated so far. It can be seen that the location of the main peak is insensitive to density, although the lifetime distribution changes shape, becoming broader and with an incipient tendency towards bimodality at high density.

The dynamics of the solvation shell around each solute molecule were studied by computing an autocorrelation function,  $\Phi(t)$ , defined as

$$\Phi(t) = \frac{\langle \delta N(t) \delta N(0) \rangle}{\langle \delta N(0) \delta N(0) \rangle} \quad (6)$$

where

$$\langle N(r) \rangle = \lim_{\tau \rightarrow \infty} \frac{1}{\tau} \int_0^{\tau} N(r,t) dt \quad (7)$$

and  $N(r,t)$  is the instantaneous number of solvent molecules located within a sphere of radius  $r$  centered around a solute molecule. Thus,  $\delta N$  is the instantaneous fluctuation of  $N(r,t)$  about  $\langle N(r) \rangle$ . Figure 9 shows the behavior of  $\Phi$  at high density, with  $r$  taken to be the distance to the first minimum of the solute-solvent pair correlation function (roughly  $2.55\sigma_{12}$ ). The autocorrelation curve is averaged over the ten solute molecules. A convenient measure of the relaxation time for the solvation shell is a time  $\tau$ , defined so that  $\Phi(\tau) = 0$  (shortest time for the vanishing of the autocorrelation). The density dependence of  $\tau$  is shown in Figure 10. The error bars show the range of values corresponding to individual solute molecules. Two features of  $\tau$  are noteworthy. First, the characteristic time for the decay of solvation shell density fluctuations is quite large (of the order tens of picoseconds). Secondly, the mean  $\tau$  shows a maximum at the solvent's critical density. Although variations among individual solute molecules are quite large, this suggests the type of dynamic sluggishness that is normally associated with critical slowing down. The origin of this effect is the growth of the correlation length and the resulting increased cooperativity. Clearly, longer simulations must be conducted in order to verify this trend.

From the molecular dynamics study we conclude that the very high solute-solute peaks do not translate to solute-solute aggregates; that the solute is present overwhelmingly in unassociated form; that this behavior is insensitive to density; that the typical lifetime of a solute dimer (0.8 ps) is insensitive to a four-fold bulk density change; and that the characteristic time for density fluctuations within the solvation shell of a solute molecule is quite long, of the order of tens of picoseconds.

#### 4. Current and Future Work

We are extending the molecular dynamics studies to higher temperatures. We plan to initiate molecular dynamics simulations of molecular fluids, and to begin the planned collaboration with Dr. James Gord, of the Systems Research Laboratory in Dayton, who

will be investigating supercritical solvation dynamics experimentally using an Ultrafast Laser System. Initially, we will study solvation and rotation dynamics in the benzene-carbon dioxide system at high solute dilution and supercritical conditions with respect to the solvent carbon dioxide).

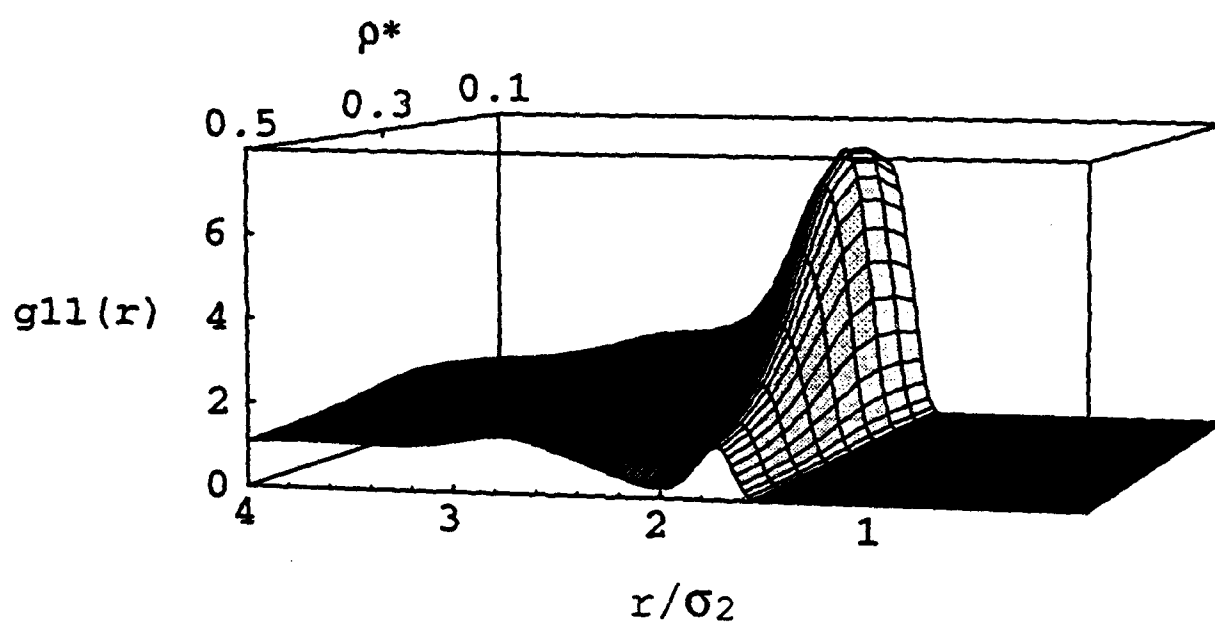


**Figure 1:** Density dependence of the solute-solute pair correlation function for the naphthalene-carbon dioxide system at  $T^* = 1.4$  and  $y_1 = 10^{-9}$ .



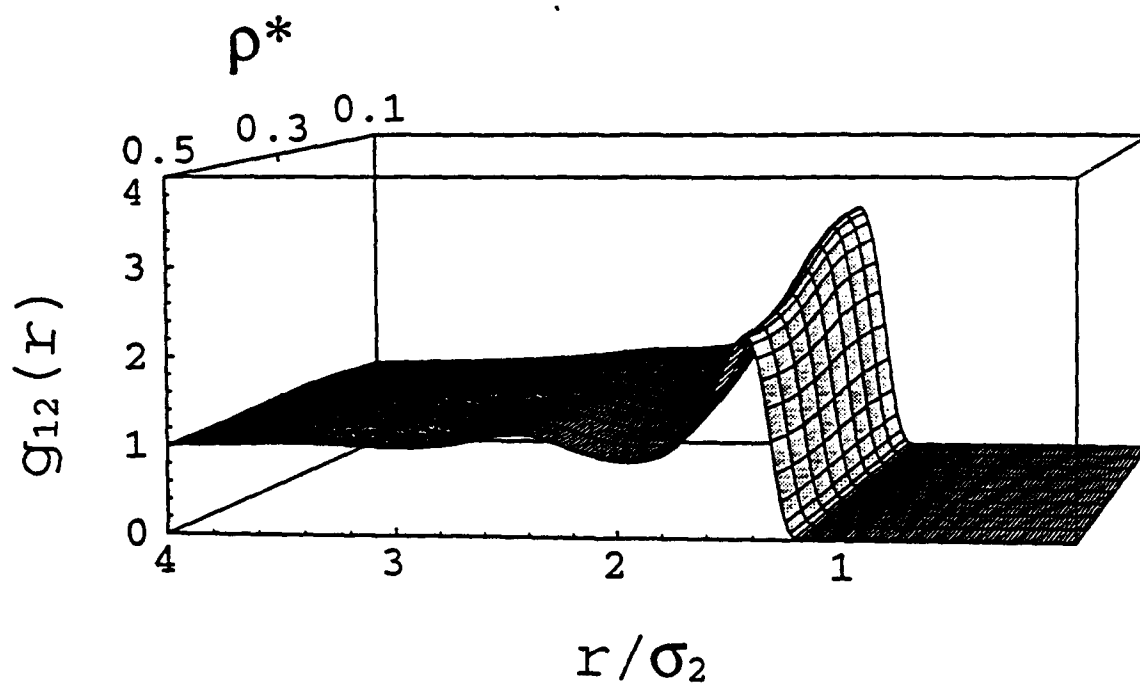


**Figure 2:** Density dependence of the solute-solvent pair correlation function for the naphthalene-carbon dioxide system at  $T^* = 1.4$  and  $y_1 = 10^{-9}$ .

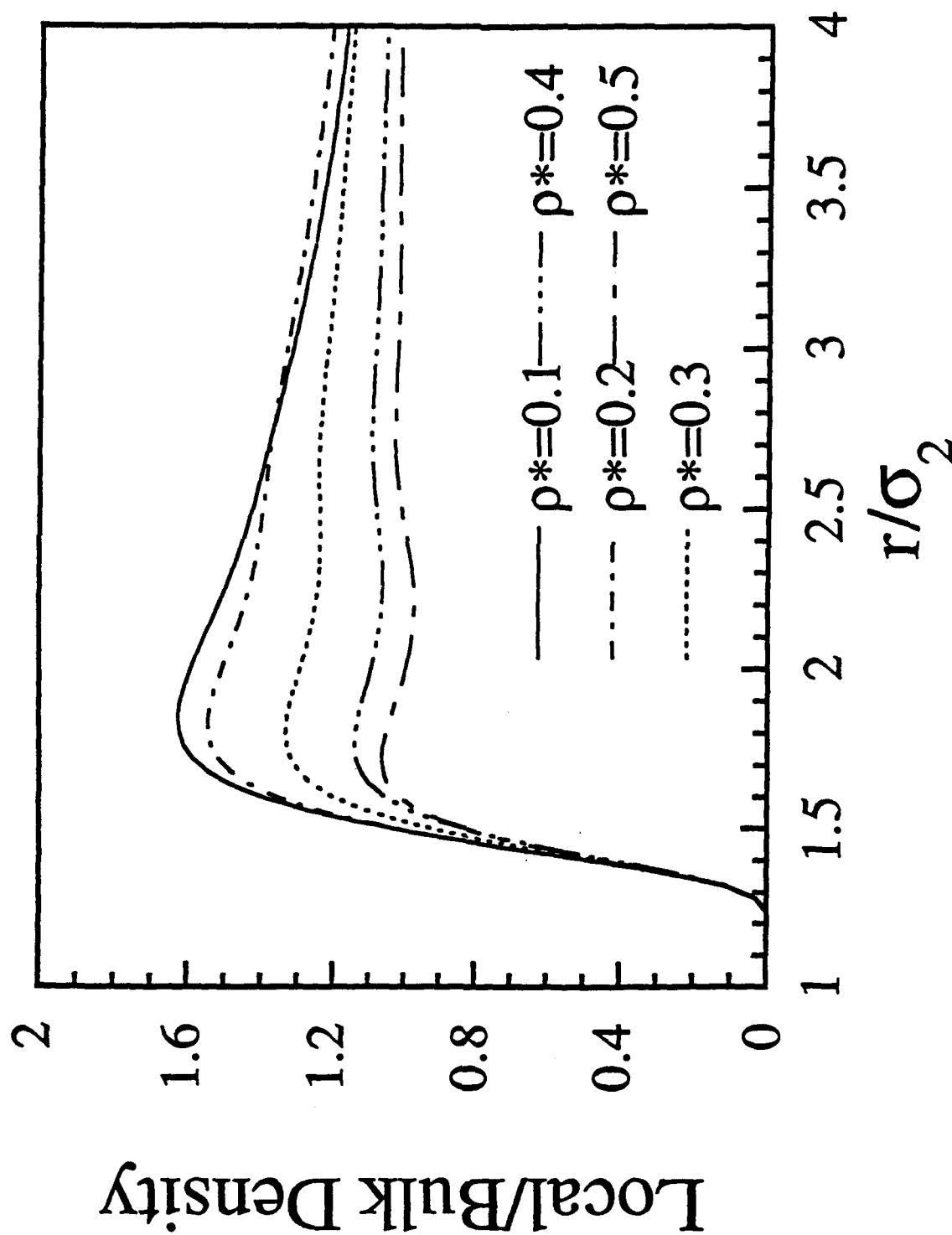
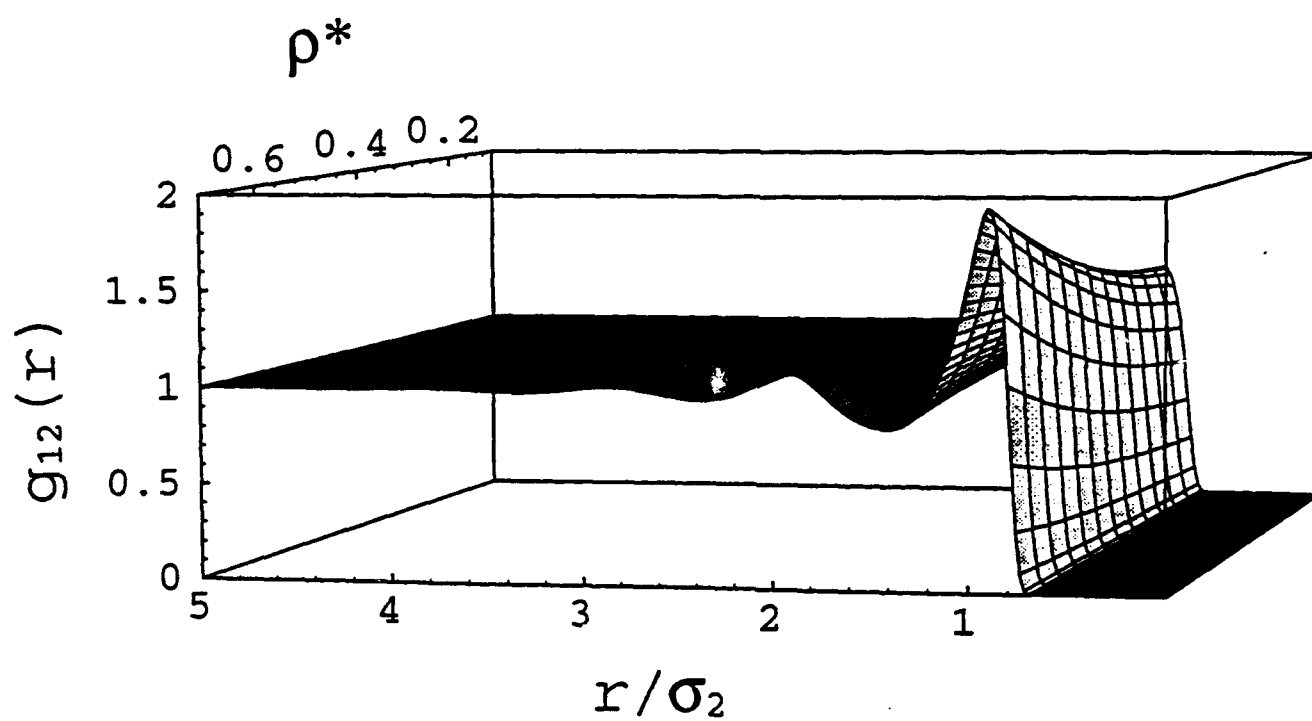
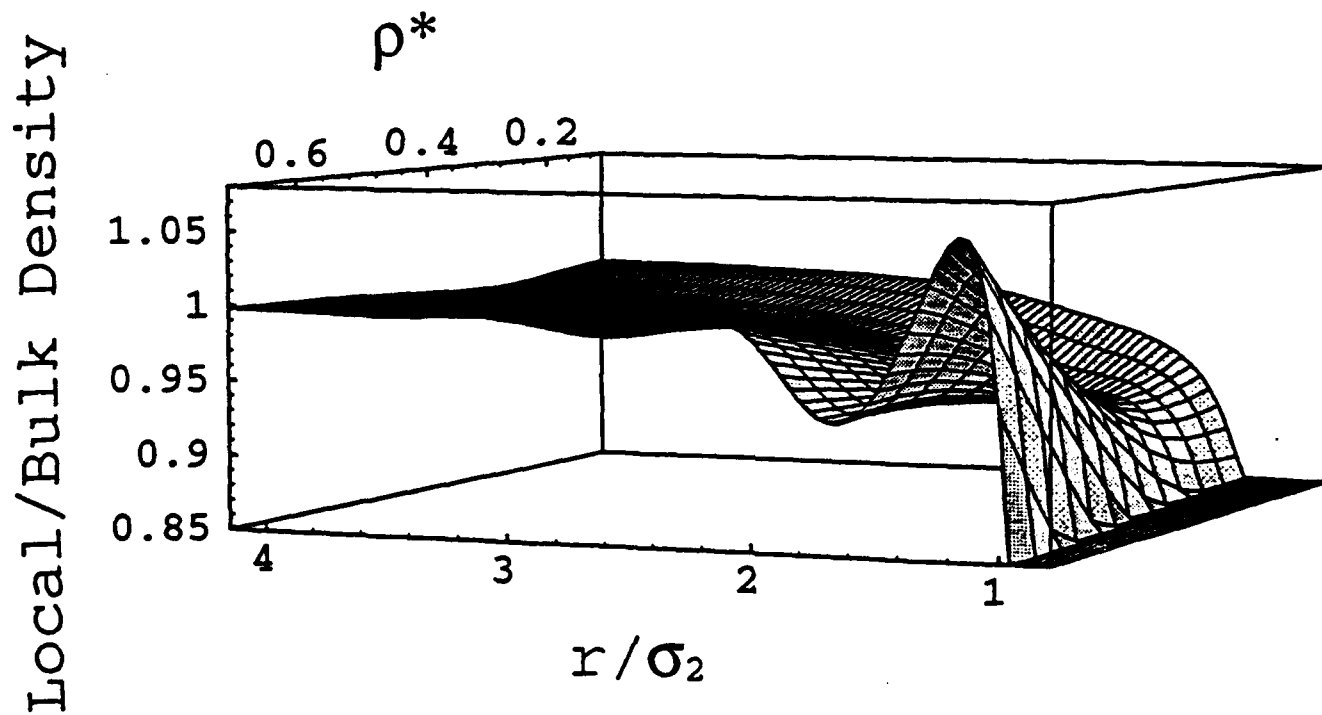


Figure 3: Radial dependence of the ratio of local-to-bulk density for the naphthalene-carbon dioxide system at  $T^* = 1.4$  and  $y_1 = 10^{-9}$ .



**Figure 4:** Density dependence of the solute-solvent pair correlation function for the neon-xenon system at  $T^* = 1.4$  and  $y_1 = 10^{-9}$ .



**Figure 5:** Three-dimensional representation of the radial dependence of the ratio of local-to-bulk density for the neon-xenon system at  $T^* = 1.4$  and  $y_1 = 10^{-9}$ .

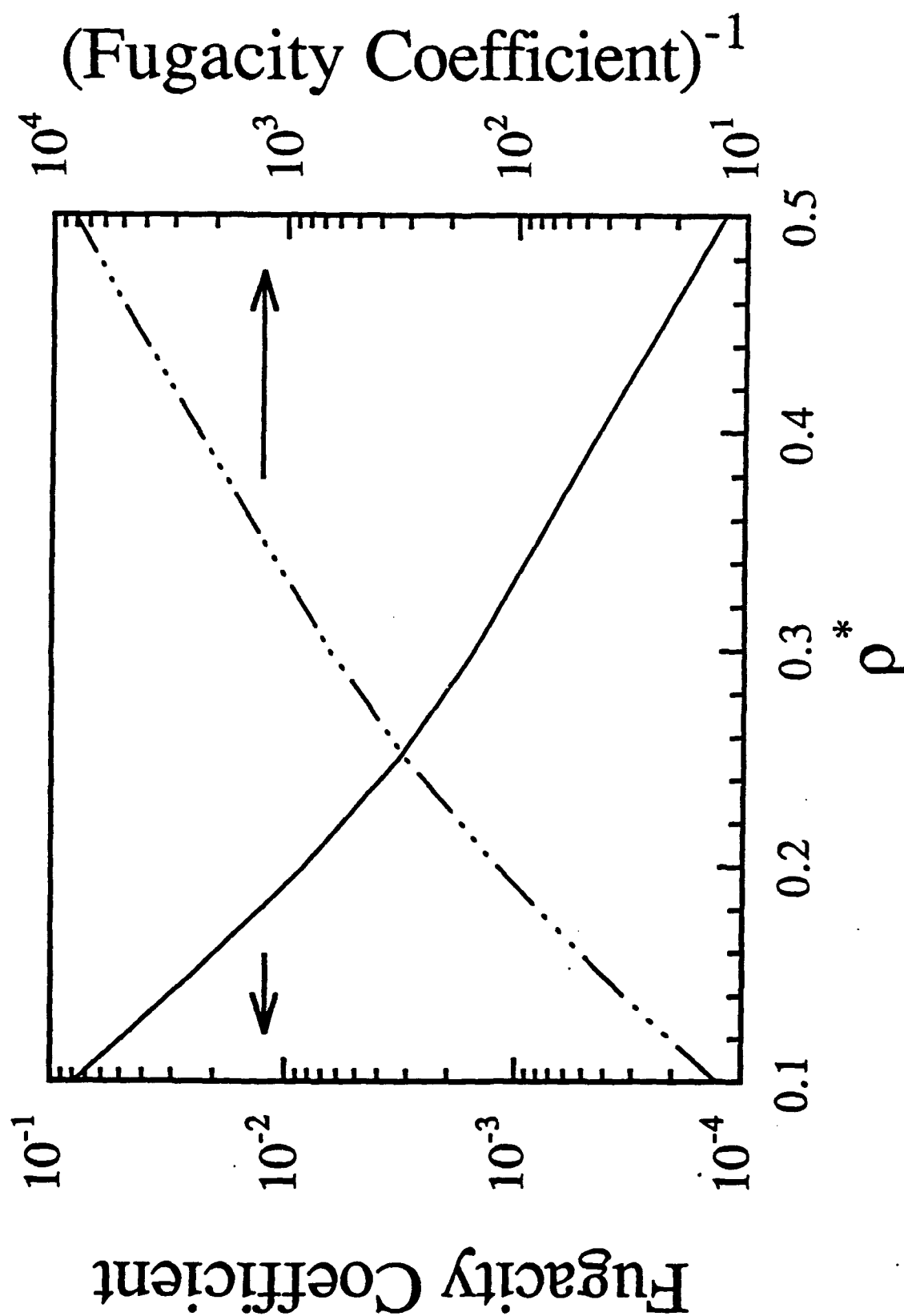


Figure 6: Density dependence of the solute's fugacity coefficient and its reciprocal for the naphthalene-carbon dioxide system at  $T^* = 1.4$  and  $y_1 = 10^{-9}$ .

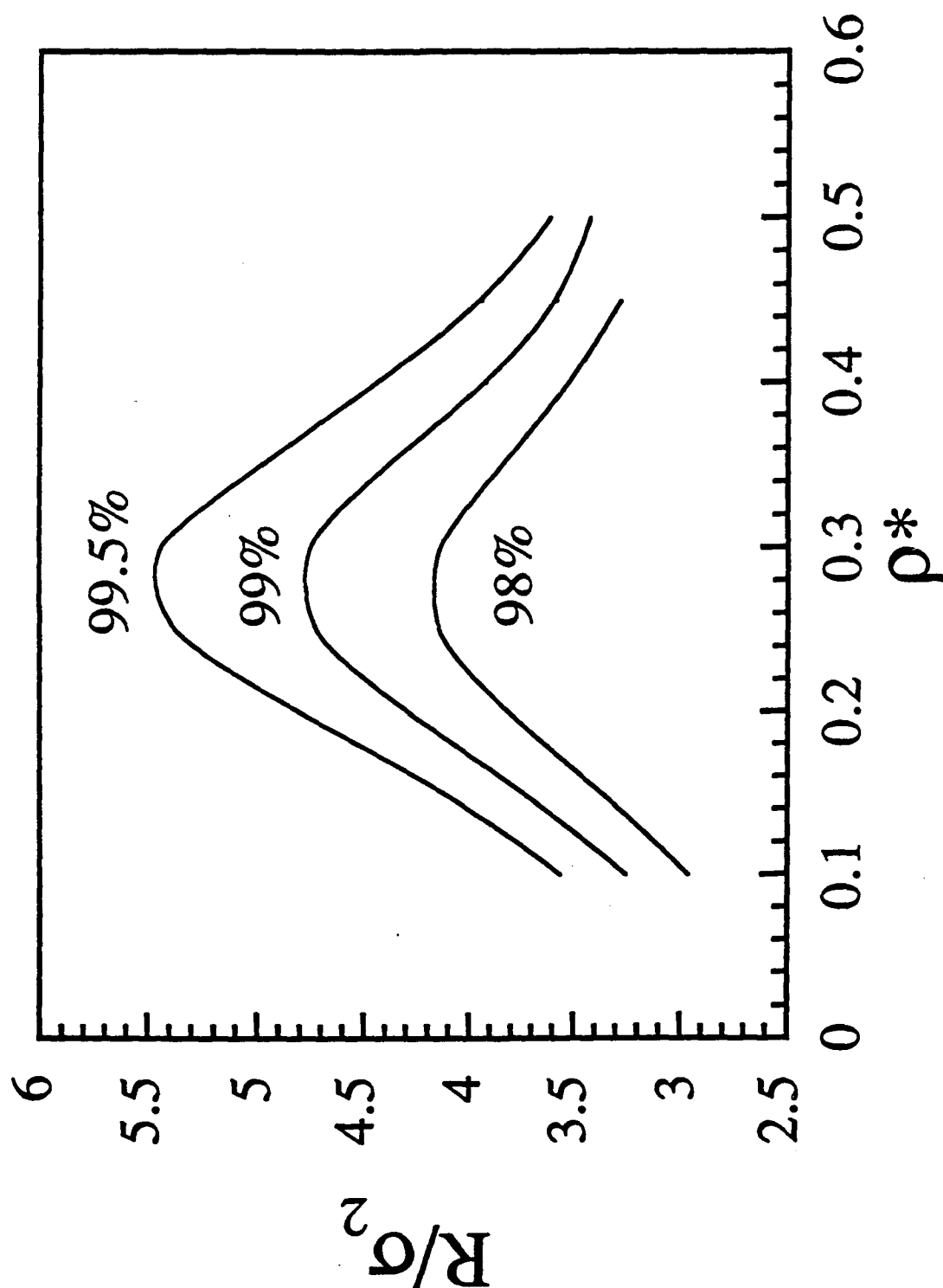
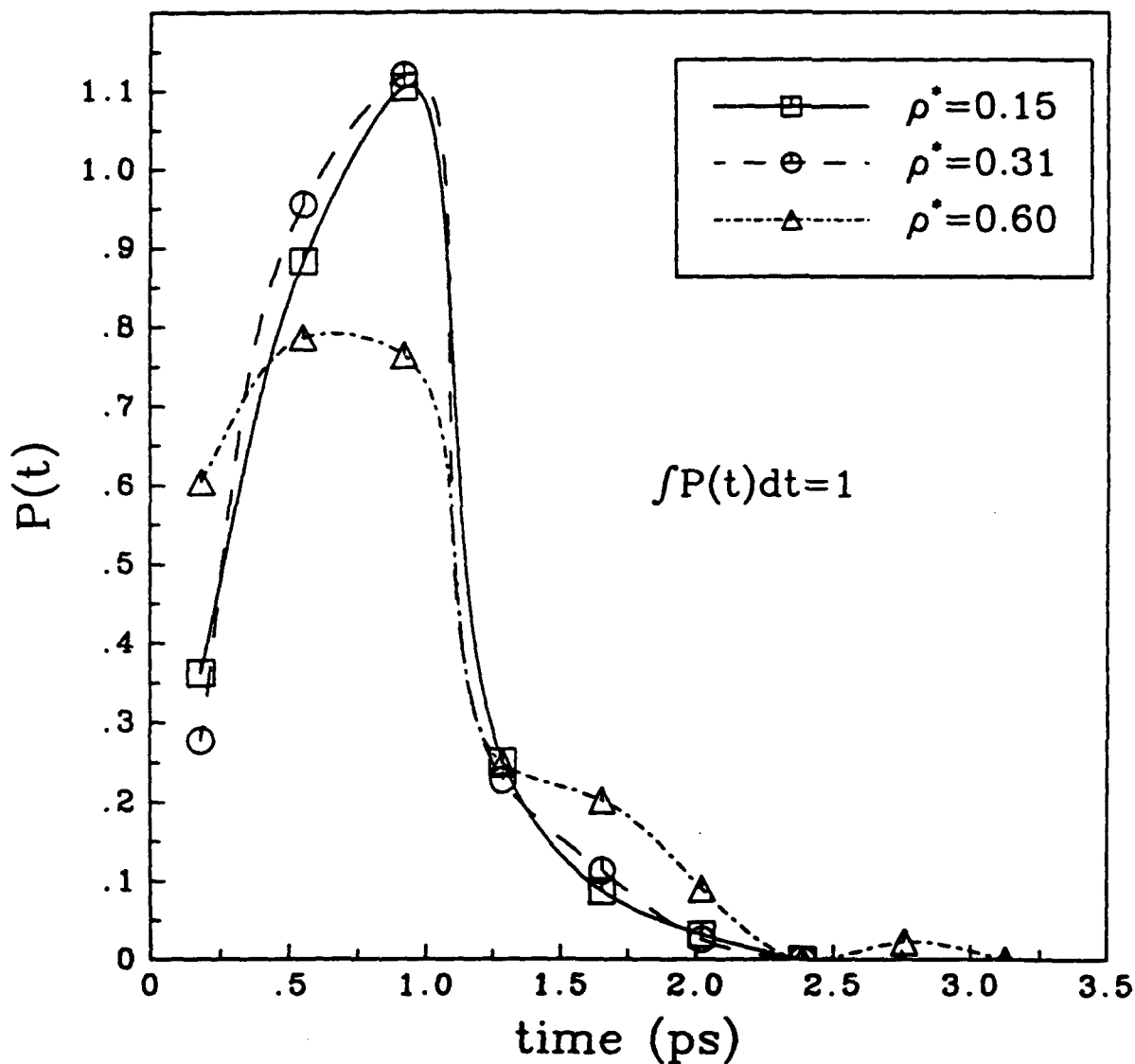


Figure 7: Density dependence of the cutoff distance (beyond which the mixture is assumed to be homogeneous) needed to obtain 98%, 99%, and 99.5% of the asymptotic solution fugacity coefficient for the naphthalene-carbon dioxide system at  $T^* = 1.4$  and  $y_1 = 10^{-9}$ .

# Distribution of Dimer Lifetimes

$N=4000$ ,  $N_1=10$ ,  $T^*=1.4$



**Figure 8:** Distribution of dimer lifetimes for the pyrene-carbon dioxide system at  $T^* = 1.4$  and  $y_1 = 0.0025$ .

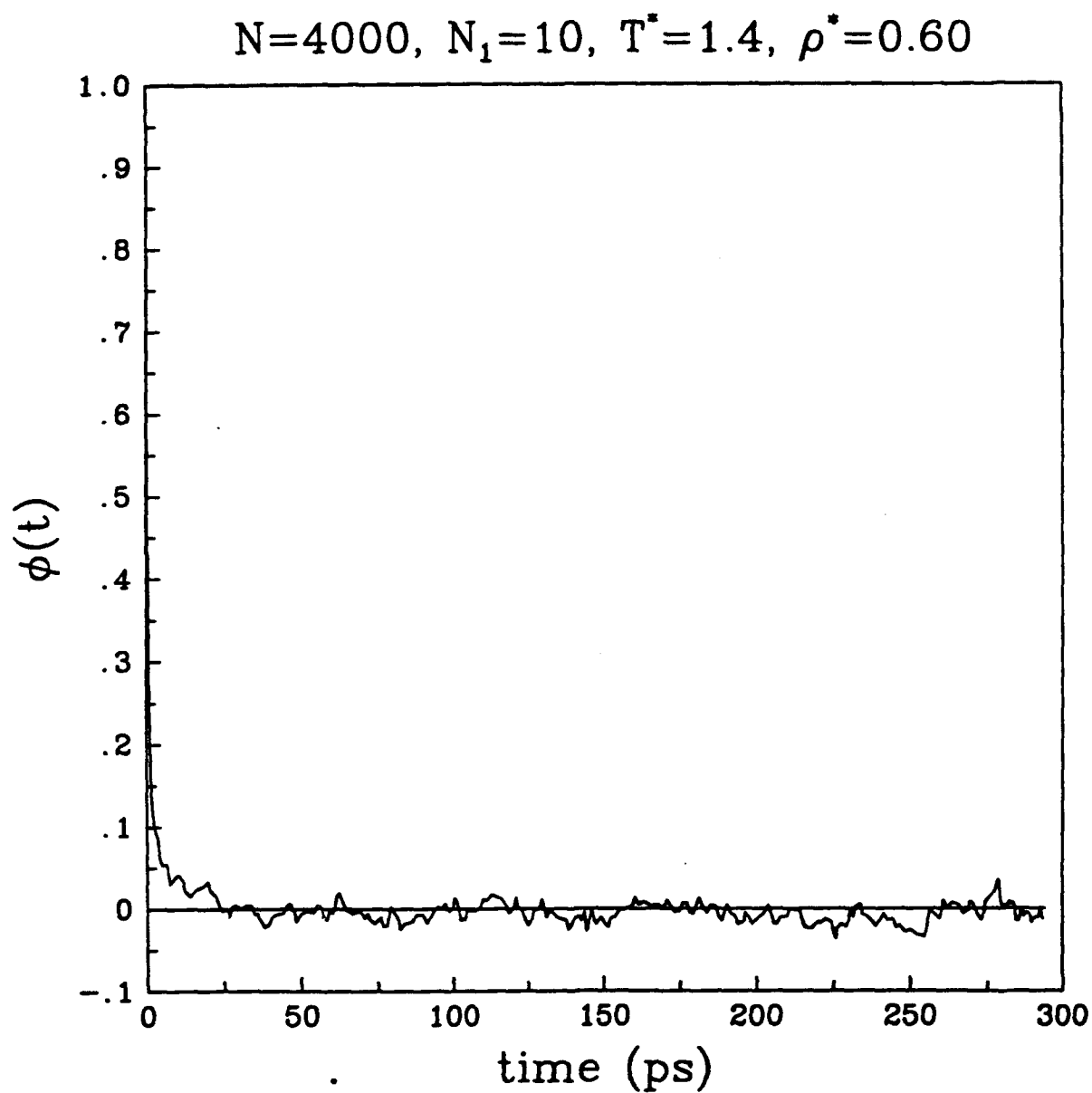


**Figure 9:** Behavior of the solvation shell autocorrelation for the pyrene-carbon dioxide system at  $T^* = 1.4$ ,  $\rho^* = 0.6$ , and  $y_1 = 0.0025$ .



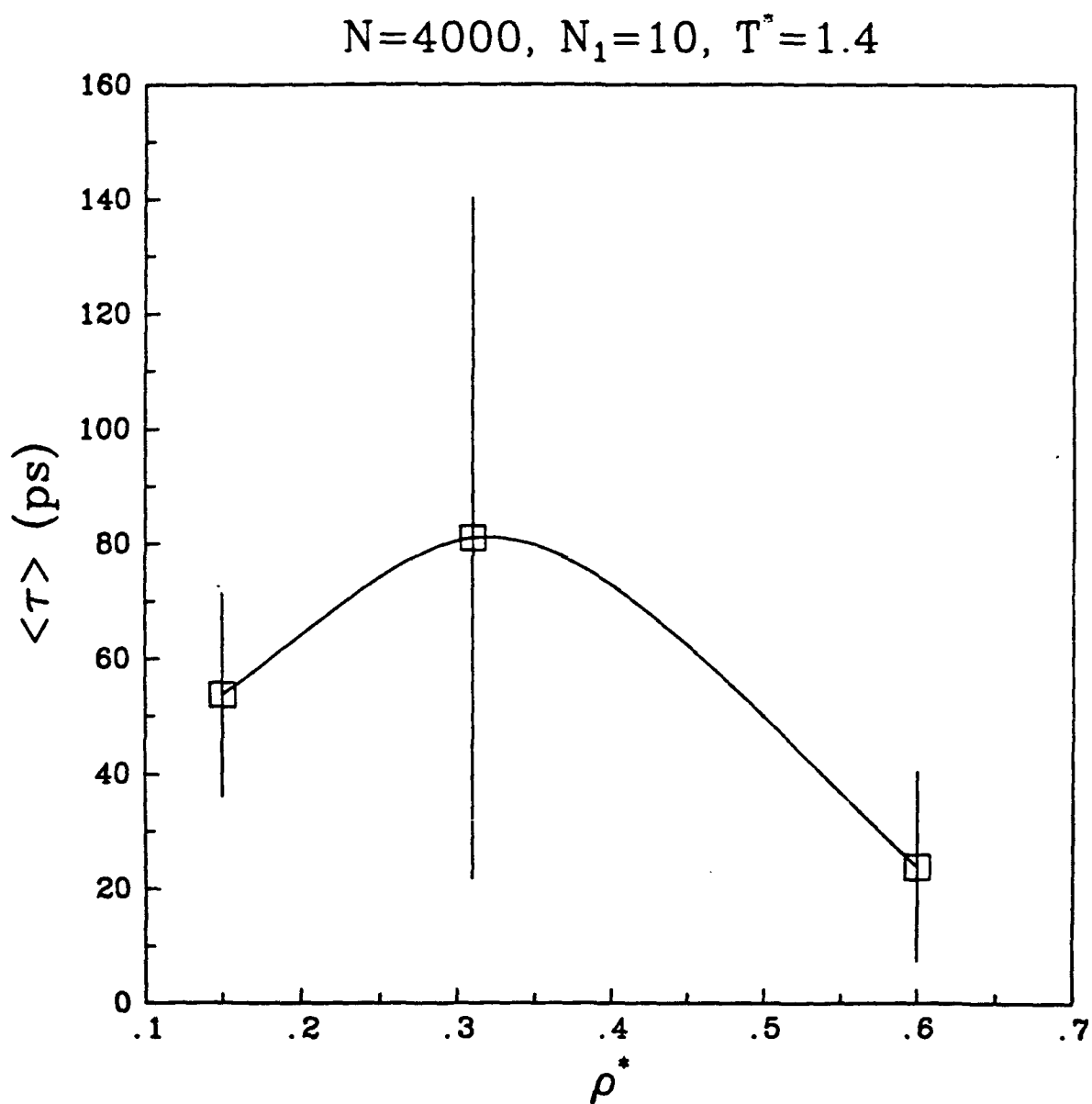


**Figure 10:** Density dependence of the characteristic time for the decay of a solvation shell density fluctuation for the pyrene-carbon dioxide system at  $T^* = 1.4$ , and  $y_1 = 0.0025$ .

## Articles

"Integral Equation Study of Microstructure and Solvation in Model Attractive and Repulsive Supercritical Mixtures". *Ind. Eng. Chem. Res.*, 32, 2118, 1993; with J.W. Tom.

"Solute-Solute Interactions: Theory and Simulations". *NATO ASI - Supercritical Fluids, Fundamentals for Application*, E. Kiran and J.M.H. Levelt-Sengers, eds. Kluwer Academic Publishers, in press, 1994.

## Presentations

"Solvation, Nucleation, and Particle Formation in Supercritical Fluids". Fuel Science Program, Dept. of Materials Science, Pennsylvania State University, University Park, April 16, 1993.

"Supercritical Fluids: Fundamentals and Applications". Sixth International Congress on Engineering and Food, Chiba, Japan, May 26, 1993.

"Solute-Solute Interactions in Supercritical Solutions: a Molecular Dynamics Investigation". Symposium on Scientific Research on Supercritical Fluids, University of Tokyo, Tokyo, Japan, May 31, 1993.

"Solute-Solute Interactions: Theory and Simulations". NATO Advanced Study Institute on Supercritical Fluids: Fundamentals for Application, Kemer, Turkey, July 22, 1993.

"Molecular Dynamics Study of Solute-Solute Interactions in Dilute Supercritical Mixtures". AIChE Annual Meeting, St. Louis, MO, November 10, 1993.

## Personnel

David S. Corti; graduate student.

Pablo G. Debenedetti; Associate Professor. Principal Investigator.

## Literature Cited

- Betts, T.A.; J. Zagrobelny; and F.V. Bright, *J. Am. Chem. Soc.*, **114**, 8163 (1992a).
- Betts, T.A.; J. Zagrobelny; and F.V. Bright, *ACS Symp. Ser.*, **488**, 48 (1992b).
- Biggerstaff, D.R., and R.H. Wood, *J. Phys. Chem.*, **92**, 1988 (1988a).
- Biggerstaff, D.R., and R.H. Wood, *J. Phys. Chem.*, **92**, 1994 (1988b).
- Brennecke, J.F., and C.A. Eckert, *AIChEJ.*, **35**, 1409 (1989).
- Brennecke, J.F.; D.L. Tomasko; J. Peshkin; and C.A. Eckert, *Ind. Eng. Chem. Res.*, **29**, 1682 (1990a).
- Brennecke, J.F.; D.L. Tomasko; and C.A. Eckert, *J. Phys. Chem.*, **94**, 7692 (1990b).
- Chialvo, A.A., and P.G. Debenedetti, *Comp. Phys. Commun.*, **64**, 15 (1991).
- Chialvo, A.A., and P.G. Debenedetti, *Ind. Eng. Chem. Res.*, **31**, 1391 (1992).
- Cochran, H.D., and L.L. Lee, *ACS Symp. Ser.*, **406**, 27 (1989).
- Debenedetti, P.G., and R.C. Reid, *AIChEJ.*, **32**, 3024 (1986).
- Johnston, K.P.; S. Kim; and J. Combes, *ACS Symp. Ser.*, **406**, 52 (1989).
- Kim, S., and K.P. Johnston, *AIChEJ.*, **33**, 1603 (1987a).
- Kim, S., and K.P. Johnston, *Ind. Eng. Chem. Res.*, **26**, 1207 (1987b).
- Knutson, B.L.; D.L. Tomasko; C.A. Eckert; P.G. Debenedetti; and A.A. Chialvo, *ACS Symp. Ser.*, **488**, 60 (1992).
- McHugh, M., and V.J. Krukonis, *Supercritical Fluid Extraction - Principles and Practice*, Butterworths: Boston (1986).
- Munoz, F., and E.H. Chimowitz, *Fluid Phase Equil.*, **71**, 327 (1992).
- O'Brien, J.; T.W. Randolph; C. Carlier; and G. Shankar, *AIChEJ.*, **39**, 1061 (1993).
- Petsche, I.B., and P.G. Debenedetti, *J. Chem. Phys.*, **91**, 7075 (1989).
- Petsche, I.B., and P.G. Debenedetti, *J. Phys. Chem.*, **95**, 386 (1991).
- Sevick, E.M.; P.A. Monson; and J. Ottino, *J. Chem. Phys.*, **88**, 1198 (1988).
- Smit, B.; P. De Smedt; and D. Frenkel, *Mol. Phys.*, **68**, 931 (1989).
- Sun, Y.; M.A. Fox; and K.P. Johnston, *J. Am. Chem. Soc.*, **114**, 1187 (1992).

Tom, J. W., and P.G. Debenedetti, *J. Aerosol Sci.*, 22, 555 (1991).

Tom, J.W., and P.G. Debenedetti, *Ind. Eng. Chem. Res.*, 32, 2118 (1993).

Wu, R.S.; L.L. Lee; and H.D. Cochran, *Ind. Eng. Chem. Res.*, 29, 977 (1990).